Spectrum Sharing SDMA with Limited Feedback: Throughput Analysis

Han-Shin Jo
Dept. Of Electronics and Control Engineering, Hanbat National University
Daejeon, Korea
[e-mail: hsjo@hanbat.ac.kr]
*Corresponding author: Han-Shin Jo

Received August 21, 2012; revised November 9, 2012; accepted December 5, 2012; published December 27, 2012

Abstract

In the context of effective usage of a scarce spectrum resource, emerging wireless communication standards will demand spectrum sharing with existing systems as well as multiple access with higher spectral efficiency. We mathematically analyze the sum throughput of a spectrum sharing space-division multiple access (SDMA) system, which forms a transmit null in the direction of other coexisting systems while satisfying orthogonal beamforming constraints. For a large number of users N, the SDMA throughput scales as $\log N$ at high signal-to-noise ratio (SNR) ($(J-1)\log\log N$ at normal SNR), where J is the number of transmit antennas. This indicates that multiplexing gain of the spectrum sharing SDMA is $\frac{J-1}{J}$ times less than that of the non-spectrum sharing SDMA only using orthogonal beamforming, whereas no loss in multiuser diversity gain. Although the spectrum sharing SDMA always has lower throughput compared to the non-spectrum sharing SDMA in the non-coexistence scenario, it offers an intriguing opportunity to reuse spectrum already allocated to other coexisting systems.

Keywords: Asymptotic throughput scaling, space-division multiple access (SDMA), spectrum sharing, precoding, feedback overhead, null-steering

http://dx.doi.org/10.3837/tiis.2012.12.012

1. Introduction

The increasing demand for wireless services has induced recent radio spectrum shortages. Given that spectrum is limited and is a scare natural resource, it should be used to its fullest. Emerging wireless networks, such as cognitive radio, femtocells, and heterogeneous networks, require spectrum sharing with other existing systems as well as higher throughput [1][2][3][[4]. Specifically, at the World Radio Communication Conference 2007 (WRC-07), the 3400-3600 MHz band was identified for use by the International Mobile Telecommunications (IMT)-Advanced system. However, the band was already allocated or is under consideration for Fixed Wireless Service such as Fixed Service, Fixed Satellite Service, or Fixed Wireless Access in many countries around the world [5]. Furthermore, the IMT-Advanced system requires higher data rates: Approximately 100 Mbps and 1 Gbps with high mobility and low mobility for 100 MHz bandwidth, respectively [6]. In Gaussian MIMO broadcast channels, simultaneous transmission to multiple users, known as multi-user MIMO or space division multiple access (SDMA), is capable of achieving very high throughput. SDMA is as a candidate for Long Term Evolution (LTE)-Advanced and IMT-Advanced standard [7]. This paper particularly focuses on an SDMA that allows spectrum sharing with other coexisting systems.

1.1 Related Work

Spectrum sharing in the coexistence scenario. Spectrum sharing is possible by the sufficient separation of radio resource dimensions in time, frequency, and space; that is, a wireless communication system adjusts resources, such as the transmit power [2][8], frequency [9], and null-steering [10][11]. Multiple antenna arrays using null-steering can protect other existing systems without additional radio resources in frequency or time. Null-steering is used to avoid radiating interference in a known direction of a victim system [11]. When the null-steering is employed at a base station (BS), no downlink throughput gain is obtained from multiple antennas owing to focusing on mitigation of interference to a victim system. As such, besides null-steering, a scheme for achieving high data rate is required to the multiple antenna systems.

Cognitive radio, a typical spectrum sharing system, has been developed. Resource management for spectrum sharing was studied in many previous works, where adaptive time and power allocation [12], joint rate and power control [13], and joint channel and power allocation [14] are considered. Moreover, ergodic capacity was theoretically analyzed in [15][16].

Throughput improvement in the non-coexistence scenario. Dirty paper coding (DPC) is capacity achieving for the MIMO broadcast channel [17]; however, it is non-causal scheme that has yet to be implemented in practical systems, thus spurring the growth of practical SDMA [18] [19]. In the industry, a codebook-based orthogonal beamforming SDMA has been proposed for the 3GPP-LTE standard [20] under the name per-user unitary rate control (PU^2RC) and has been included in the 3GPP2-ultra mobile broadband (UMB) standard [16]. In this scheme, on the basis of limited feedback information on the preferred precoding matrices within a codebook and the corresponding signal-to-interference-and-noise ratios (SINRs), the multiuser precoding matrix is selected within a codebook to maximize the sum throughput. More detailed study of PU2RC is given in [22][23]. Recently, the performance of PU2RC with mode switching has been studied in [24]. The orthogonal beamforming of

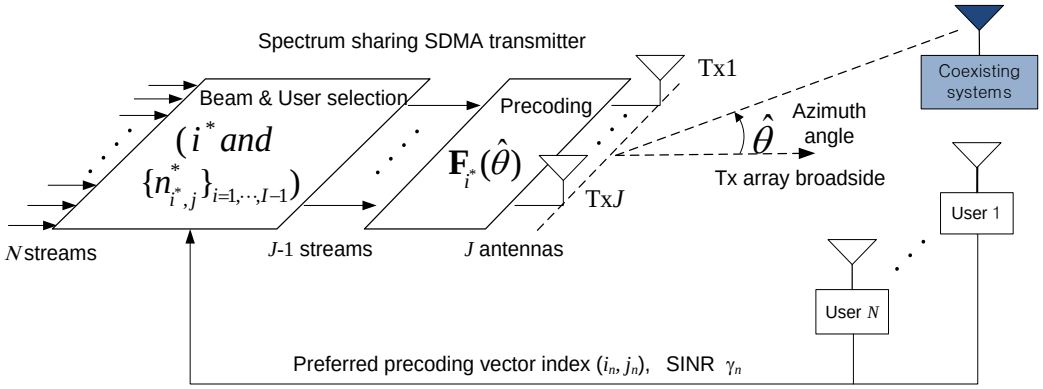

Fig. 1. Spectrum sharing SDMA system.

PU^{2}RC focuses on throughput improvement on the basis of inter-user interference mitigation in homogeneous systems. However, such non-coexisting SDMA systems are useless in the coexistence scenario, because they are required to suppress interference between the heterogeneous systems as well as the inter-user interference in homogeneous systems.

Achieving both spectrum sharing and high data rate in the coexistence scenario. Integrating orthogonal beamforming and null-steering is a promising solution for achieving both spectrum sharing (i.e. *mitigating interference to other coexisting systems*) and high throughput. A part of spatial transmission resources provided by multiple antennas are employed for spectrum sharing instead of data transmission. This concept is realized by designing a SDMA precoder that satisfies both null-steering and orthogonality constraints, where the matrix comprises $J-1$ (J denotes the number of transmit antennas) mutually orthonormal vectors that are orthogonal to the array steering vector in the direction of coexisting systems [25]. We call such SDMA *spectrum sharing SDMA*. Although the spectrum sharing SDMA offers an opportunity to reuse spectrum allocated to other systems, it should have lower throughput compared to the orthogonal beamforming SDMA, i.e. PU^{2}RC, in the non-coexistence scenario. The aim of this paper is to quantify the throughput of the spectrum sharing SDMA and the required feedback overhead, and to compare them with PU^{2}RC.

1.2 Contributions and Organization

We use spectrum sharing codebook comprising multiple sets of orthonormal vectors, and multiuser scheduling with limited feedback. The codebook satisfying null-steering and orthogonal beamforming constraints is deterministically generated on the Gram-Schmidt process. The main contribution of this paper is to derive throughput scaling laws for the spectrum sharing SDMA. We preliminarily derive the statistics of channel-shape quantization error. Then, we derive throughput scaling laws on the basis of extreme value theory [18] and uniform convergence in the weak law of large numbers [22]. Finally, the multiplexing gain and the multiuser diversity gain of the spectrum SDMA are quantified.

The remainder of this paper is organized as follows. The system model is described in Section 2. Section 3 presents the asymptotic throughput analysis. In Section 4, numerical results are discussed. Finally, conclusions are presented.

2. System Model

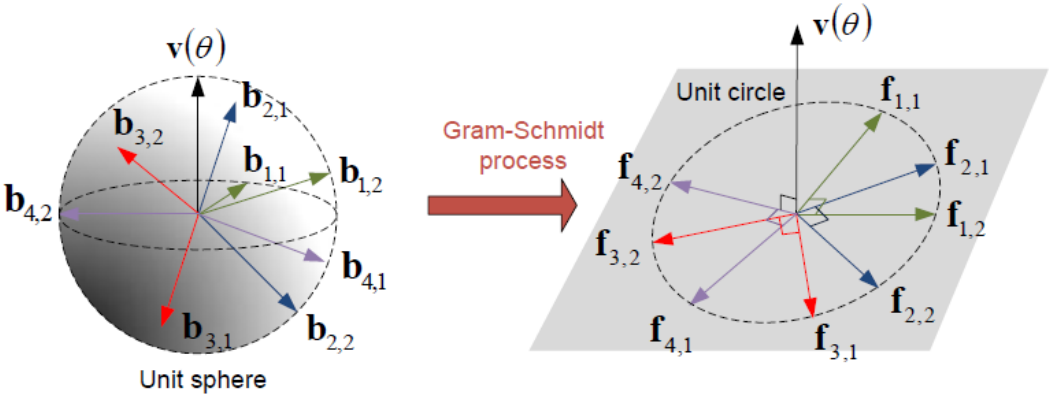

Fig. 2. An array steering vector $\mathbf{v}(\theta)$ at θ and precoding vectors $\{[\mathbf{f}_{1,1}, \mathbf{f}_{1,2}], [\mathbf{f}_{2,1}, \mathbf{f}_{2,2}], [\mathbf{f}_{3,1}, \mathbf{f}_{3,2}], [\mathbf{f}_{4,1}, \mathbf{f}_{4,2}], \}$ for $I = 4$, $J = 3$, $M = 12$. All vectors have unit length. Two precoding vectors comprising a precoding matrix are mutually orthonormal. Every precoding vector is orthonormal to the array steering vector.

We assume a downlink SDMA system, which consists of a transmitter with J antennas and N receivers (users) with one antenna. The system operates in the spectrum owned by other coexisting systems, and it forms $J-1$ orthonormal beams and transmits to $J-1$ scheduled users via the precoding vectors $\{\mathbf{f}_j\}_{j=1,\cdots,J-1}$. We assume flat Rayleigh fading channel from the transmitter to the n-th user. Let $\mathbf{x} \in \mathbb{C}^{N\times 1}$ be a transmit symbol vector. Then, the received signal of the n-th user is given by

$$y_n = \mathbf{h}_n \mathbf{x} + z_n \,, \tag{1}$$

where $\mathbf{h}_n \in \mathbb{C}^{1\times J}$ is channel gain vector with zero mean unit variance, and z_n is an additive noise with unit variance complex Gaussian noise vector. An SDMA system is considered that constructs $J-1$ orthonormal beams and transmits to $J-1$ scheduled users via the precoding vector $\{\mathbf{f}_j\}_{j=1,\cdots,J-1}$. The transmit signal is then

$$\mathbf{x} = \mathbf{F}\mathbf{s} = \textstyle\sum_{j=1}^{J-1} \mathbf{f}_j s_j, \tag{2}$$

where $\mathbf{F} = [\mathbf{f}_1 \cdots \mathbf{f}_{J-1}] \in \mathbb{C}^{J\times J-1}$ is the precoding matrix, and $\mathbf{s} = [s_1 \cdots s_{J-1}]^T$ is the transmit symbol vector with $\mathbb{E}\{\|\mathbf{s}\|^2\} = P$. The total transmit power P is equally allocated over $J-1$ scheduled users. Since the average noise power is assumed to be one, P represnts the average signal-to-noise ratio (SNR). The precoding matrix $\mathbf{F}$ is selected within a precoder codebook $\mathcal{F} = \{\mathbf{F}_i\}_{i=1,\cdots I}$ using the beam and user selection algorithm described in the latter part of this Section. We assume that the channel gain vector $\mathbf{h}_n$ has uncorrelated complex Gaussian entries. The investigation for a correlated channel model is left to future work. Unlike $\mathbf{h}_n$, we assume the highly correlated channel from the transmitter to other coexisting systems on the basis of high line-of-sight probability between them. It facilitates mitigating interference to other coexisting systems by construction of transmit null at the transmitter.

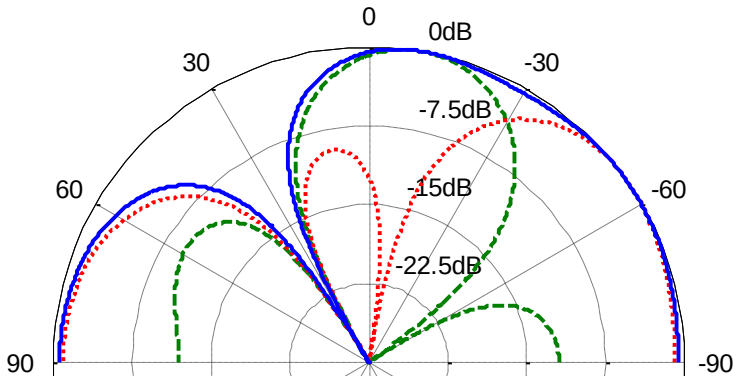

Fig. 3. Transmit gain (blue solid line) of a precoding matrix $\mathbf{F}_1 = [\mathbf{f}_{1,1}, \mathbf{f}_{1,2}]$, $\mathbf{f}_{1,1} = [0.5774, 0.5297 + 0.2298j, 0.3452 + 0.4628j]^{\mathrm{T}}, \mathbf{f}_{1,2} = [0.5774, -0.4638 + 0.3438j, 0.2281 - 0.5304j]^{T}$, where $\mathbf{v}(\theta = 30°) = [0.5774, 0.5774j, -0.5774]^{\mathrm{T}}, I = 1, J = 3$. The red and green dashed line is the transmit gain of $\mathbf{f}_{1,1}$and $\mathbf{f}_{1,2}$, respectively. The precoding matrix forms a transmit-null at $\theta = 30°$.

Although LOS is not guaranteed, the angle spread (AS) of the channel in realty is not so large; that is, the mean AS ranges from 5 deg to 19 deg as shown in [26]. This indicates that the coexisting systems are mainly interfered by the transmitter signal radiated in a certain direction θ within a small range. The transmitter can obtain the θ by adopting adopting a popular spatial-spectrum estimation direction-finding method [27][28] or from a database with the θ. Thus, when the LOS is not guaranteed, it is desirable to form the transmit-null at the θ instead of the LOS direction.

2.1 Codebook

We consider a precoder codebook $\mathcal{F} = \{\mathbf{F}_i\}_{i=1,\cdots,I}$, where I denotes the number of precoding matrices, and each precoding matrix consists of $J-1$ column (precoding) vectors as $\mathbf{F}_i = \left[f_{i,1}, \cdots, f_{i,J-1}\right] \in \mathbb{C}^{J \times J-1}$. Thus, the codebook is of size $K = I(J-1)$. In order to support SDMA and suppress interference to other coexisting systems, the spectrum sharing SDMA transmitter adaptively constructs the precoding matrices forming a transmit-null in the azimuth direction angle $\hat{\theta}$ of the other coexisting system, while satisfying orthogonal beamforming constraint. The angle $\hat{\theta}$ is relative to the array boradside of the spectrum sharing transmitter, as shown in **Fig. 1**. The codebook design principle for the above requirements is presetend in the sequel.

First, to support orthogonal beamforming, the precoding matrices $\{\mathbf{F}_i\}_{i=1,\cdots,I}$ are unitary; that is, the $J-1$ precoding vectors in each matrix are mutually orthonormal. Second, to present the method of the transmit-null construction, we define a transmit gain. The transmit gain of a precoding maxtrix $\mathbf{F}_i = \left[\mathbf{f}_{i,1}, \cdots, \mathbf{f}_{i,J-1}\right]$ at a azimuth direction angle θ relative to the array broadside is defined as

$$G(\mathbf{F}_i, \theta) \triangleq \sum_{j=1}^{J-1} |\mathbf{f}_{i,j}^{T} \mathbf{v}(\theta)|^2, \tag{3}$$

where $\mathbf{v}(\theta)=\frac{1}{\sqrt{J}}\left[1e^{\sqrt{-1}2\pi\frac{d}{\lambda}sin\theta}\cdots e^{\sqrt{-1}2\pi(J-1)\frac{d}{\lambda}sin\theta}\right]^T$ is the array steering vector at θ, and $(\cdot)^{\mathrm{T}}$ denotes the transpose matrix operation. Also in the same manner, the transmit gain of a precoding vector is given by

$$G\left(\mathbf{f}_{i,j},\theta\right)=|\mathbf{f}_{i,j}^{T}\mathbf{v}(\theta)|^2. \tag{4}$$

Thus, when the precoding matrix $\mathbf{F}_i$ forming a trasnmit-null at $\hat{\theta}$, the transmit gain is zero as follows:

$$G\left(\mathbf{F}_i,\hat{\theta}\right)=\sum_{j=1}^{J-1}|\mathbf{f}_{i,j}^{T}\mathbf{v}(\hat{\theta})|^2=0\ . \tag{5}$$

This equation indicates that the $J-1$ mutually orthonormal vectors $\left\{\mathbf{f}_{i,j}\right\}_{j=1,\cdots,J-1}$ in the precoding matrix $\mathbf{F}_i$ are orthonormal to the array steering vector at $\hat{\theta}$, $\mathbf{v}\left(\hat{\theta}\right)$, as shown in **Fig. 2**.

To do this, we first consider I linearly independent sets $\{\mathbf{B}_i\}_{i=1,\cdots,I}$, where $\mathbf{B}_i=\left[\mathbf{b}_{i,1},\cdots,\mathbf{b}_{i,N-1},\mathbf{v}\left(\hat{\theta}\right)\right]\in\mathbb{C}^{J\times J}$. The I orthonormal sets $\{\mathbf{U}_i\}_{i=1,\cdots,I}$, where $\mathbf{U}_i=\{\mathbf{f}_{i,1},\cdots,\mathbf{f}_{i,J-1},\mathbf{v}(\hat{\theta})\}\in\mathbb{C}^{J\times J}$, are then generated from $\{\mathbf{B}_i\}_{i=1,\cdots,I}$ using the Gram-Schmidt process, as shown in **Fig. 2**. Finally, the desired precoding matrix $\mathbf{F}_i=[\mathbf{f}_{i,1}\cdots\mathbf{f}_{i,J-1}]\in\mathbb{C}^{J\times J-1}$ is given by deleting the last column vector $\mathrm{v}\left(\hat{\theta}\right)$ from $\mathrm{U_i}$. **Fig. 3** shows an example of the transmit gain of a precoding matrix F_1 and a array steering vector $\mathrm{v}\left(\hat{\theta}=30°\right)$.

2.2 Beam and User Selection with Limited Feedback

It is assumed that the n-th user has perfect receive channel state information (CSI) $\mathbf{h}_n$. Although rather unrealistic, this assumption is desirable to focus on the effects of the quantized channel shape and to secure analytical tractability as in [18][19][22][31]. From the assumption, the n-th user chooses a precoding vector in a codebook $\mathcal{F}$ with the size of $K=I(J-1)$ as follows:

$$\mathbf{f}_{i_n,j_n}=\arg\max_{\mathbf{f}_{i,j}\in\mathcal{F}}\left|\tilde{\mathbf{h}}_n\mathbf{f}_{i,j}\right|^2, \tag{6}$$

where $\tilde{\mathbf{h}}_n=\mathbf{h}_n/\|\mathbf{h}_n\|$ is a unit vector representing a channel direction. In (6), since $\left|\tilde{\mathbf{h}}_n\mathbf{f}_{i,j}\right|^2=\cos^2\left(\angle\left(\tilde{\mathbf{h}}_n,\mathbf{f}_{i,j}\right)\right)=1-\sin^2\left(\angle\left(\tilde{\mathbf{h}}_n,\mathbf{f}_{i,j}\right)\right)$, the vector $\mathbf{f}_{i_n,j_n}$ selected at the nth user minimizes the quantization error of channel shape of the nth user, which is defined as $\sin^2\varphi_n$, $\varphi_n=\angle(\tilde{\mathbf{h}}_n,\mathbf{f}_{i_n,j_n})$. Since the codebook $\mathcal{F}$ is known a priori to both BS and user, only the index i_n and j_n of the selected precoding vector is send back to a transmitter. This requires feedback bits of $\log_2 I(J-1)$. Furthermore, the n-th user reports its SINR γ_n which is

$$\gamma_n=\frac{\frac{P}{J-1}\|\mathbf{h}_n\|^2\cos^2\varphi_n}{1+\frac{P}{J-1}\|\mathbf{h}_n\|^2\sum_{j=1,j\neq j_n}^{J-1}|\tilde{\mathbf{h}}_n\mathbf{f}_{i_n,j}|^2}. \tag{7}$$

Here, we assume that the SINR is reported to the transmitter without quantization as in [18][19][22][31] to focus on the effects of the quantized channel shape. Denote $\mathbf{e}_{i_n}$ as a unit

vector orthogonal to the $J-1$ dimensional hyperplane that orthonormal bases $\{\mathbf{f}_{i_n,j}\}_{j=1,\cdots,N-1}$ span. The set $\{\mathbf{f}_{i_n,1},\cdots,\mathbf{f}_{i_n,J-1},\mathbf{e}_{i_n}\}$ forms an orthonormal basis of $\mathbb{C}^J$, and thus

$$\sum_{j=1,j\neq j_n}^{J-1}|\tilde{\mathbf{h}}_n\mathbf{f}_{i_n,j}|^2+|\tilde{\mathbf{h}}_n\mathbf{e}_{i_n}|^2+|\tilde{\mathbf{h}}_n\mathbf{f}_{i_n,j_n}|^2=1. \tag{8}$$

From (8), we obtain

$$\begin{aligned}\sum_{j=1,j\neq j_k}^{J-1}|\tilde{\mathbf{h}}_n\mathbf{f}_{i_n,j}|^2+|\tilde{\mathbf{h}}_n\mathbf{e}_{i_n}|^2&=1-|\tilde{\mathbf{h}}_n\mathbf{f}_{i_n,j_n}|^2\\&=\sin^2\varphi_n.\end{aligned} \tag{9}$$

Therefore, (7) becomes

$$\gamma_n=\frac{\frac{P}{N-1}\|\mathbf{h}_n\|^2\cos^2\varphi_n}{1+\frac{P}{N-1}\|\mathbf{h}_n\|^2(\sin^2\varphi_n-\varepsilon)}, \tag{10}$$

where $0\leq\varepsilon=|\tilde{\mathbf{h}}_n\mathbf{e}_{i_n}|^2\leq\sin^2\varphi_n\leq 1$.

According to their selected precoding vector, all N users fall into $I(J-1)$ groups accoding to their indices of the selected precoding vectors as follows:

$$\mathcal{S}_{i,j}=\{1\leq n\leq N|i_n=i,j_n=j\},1\leq i\leq I,1\leq j\leq J-1. \tag{11}$$

For each group, the transmitter selects one user with the highest SINR among $|\mathcal{S}_{i,j}|$, whose index is $n_{i,j}^*=\text{argmax}_{n\in\mathcal{S}_{i,j}}\gamma_n$ and the highest SINR is

$$\gamma_{i,j}^*=\max_{n\in\mathcal{S}_{i,j}}\gamma_n. \tag{12}$$

Then, the maximum (instantaneous) sum throughput using the i-th precoding matrix $\mathrm{F_i}$ is given by

$$\hat{R}(\mathbf{F}_i)=\sum_{j=1}^{J-1}\log\left(1+\gamma_{i,j}^*\right). \tag{13}$$

Finally, among I precoding matrices, the transmitter selects the matrix $\mathrm{F_{i^*}}$ used for transmission, which maximizes the instantaneous sum throughput in (13) as follows:

$$\hat{R}(\mathbf{F}_{i^*})=\max_{i=1,\cdots,I}\sum_{j=1}^{J-1}\log\left(1+\gamma_{i,j}^*\right). \tag{14}$$

Thereby, the scheduled users, who are specified by the indices $\{n_{i^*,j}^*\}_{j=1,\cdots,J-1}$, share the i^*th precoding matrix, which makes the feedback information on SINRs from users valid, and thus, enables the BS to exactly predict SINRs of the users. Combining (10), (12), and (14), the ergodic throughput for the spectrum sharing SDMA is given by

$$R=\mathbb{E}\left[\max_{1\leq i\leq I}\sum_{j=1}^{J-1}\log\left(1+\max_{n\in\mathcal{S}_{i,j}}\frac{\frac{P}{J-1}\|\mathbf{h}_n\|^2\cos^2\varphi_n}{1+\frac{P}{J-1}\|\mathbf{h}_n\|^2(\sin^2\varphi_n-\varepsilon)}\right)\right]. \tag{15}$$

3. Asymptotic Throughput Analysis

3.1 Preliminary Calculations

We first analyze statistical properties of the channel-shape quantization error, $\sin^2\varphi_n$, defined in previous Section. The complementary cumulative distribution function (CCDF) of $\sin^2\varphi_n$ is given as follows.

Lemma 1: *For a codebook $\mathcal{F}$ with the size of $K = I(J-1)$, the CCDF of $sin^2\varphi_n$ is given by*

$$\mathbb{P}[\sin^2\varphi_n \geq \delta] = 1 - K\delta^{J-1}, 0 \leq \delta \leq \delta_0, \tag{16}$$

where $\delta_0 = 0.5(1 - \max_{1\leq i\leq j\leq K}|\mathbf{f}_i^{\dagger} \cdot \mathbf{f}_j|)$.
Proof : See Appendix 6.1. ∎

Note that Lemma 1 contributes the CCDF of deterministically generated codebook, which is differentiated from the CCDF of random codebooks [22][30][31]. **Fig. 4** illustrates channel direction $\tilde{\mathbf{h}}_n$, its quantized channel direction f_{i_n,j_n}, and the channel-shape quantization error $\sin^2\varphi_n$. **Fig. 4** also helps to understand the proof of Lemma 1 in Appendix 6.1. Next, we derive the expectation of the logarithm of the minimum quantization error among *N* users, which is used to derive asymptotic throughput scaling law.

Lemma 2: *When Z is the mumimum of N beta $(J-1, 1)$ random variales with CCDF given by $\mathbb{P}[Z \geq z] = (1 - z^{J-1})^N$, the expectation of the logarithm of the Z , $\mathbb{E}[-\log Z]$, is bounded as*

$$\frac{\log N}{J-1} \leq \mathbb{E}[-\log Z] \leq \frac{1+\log N}{J-1}, \tag{17}$$

Proof : See Appendix 6.2.

Lemma 3: *The expectation of the logarithm of the minimum quantization error among N users using a codebook $\mathcal{F}$ with the size of $K=I(J-1)$ is bounded as*

$$\frac{\log N}{J-1} + \frac{\log K}{J-1} \leq \mathbb{E}[-\log X] \leq \frac{1+\log N}{(J-1)\tau} + \frac{\log K}{J-1}, \tag{18}$$

where $X = \min_{1\leq n\leq N}\sin^2\varphi_n$ and $\tau = \left(1 - Kx_0^{J-1}\right)^N$.
Proof : See Appendix 6.3. ∎

3.2 Asymptotic Throughput Scaling

The asymptotic scaling law is derived based on both the extreme value theory [18, Appendix A] and the uniform convergence in the weak law of large numbers [22, Lemma 1]. We first derive the asymptotic throughput scaling law of the spectrum sharing SDMA in the normal SNR regime. The results are obtained as follows.

Theorem 1: *In the normal SNR regime, the throughput of the spectrum sharing SDMA scales like*

$$\lim_{N\to\infty} \frac{R}{(J-1)\log\log N} = 1. \tag{19}$$

Proof: See Appendix 6.4. ∎

Theorem 1 states that the throughput scales linearly with the number of transmit antennas minus one, $J-1$. This indicates that when compared to a typical SDMA, i.e., PU2RC ($\lim_{N\to\infty}\frac{R}{J\log\log N}=1$) [22], the throughput the scaling law of the spectrum sharing SDMA is $(J-1)/J$ times that of PU2RC with orthogonal beamforming but no transmit-null. Thus, the spectrum sharing SDMA achieves smaller multiplexing gain, $J-1$, than PU2RC, J. This is attributed to the fact that the spectrum sharing SDMA employs one spatial degrees of freedom among total J spatial degrees of freedoms to mitigate the interference toward other coexisting services, and $J-1$ spatial degrees of freedom are devoted to send data streams. Furthermore, Theorem 1 yields that the throughput scales double logarithmically with the number of users N; that is, multiuser diversity gain increases the throughput by the factor of $\log\log N$, which is the same as PU2RC. This implies that no loss in the multiuser diversity gain is provided.

Next, we evaluate the throughput scaling law of the spectrum sharing SDMA in the high SNR regime (or interference limited regime). In the regime, the SINR (10) becomes $\frac{1-\varepsilon}{\sin^2\varphi_n-\varepsilon}$, because

$$1+\frac{\frac{P}{J-1}\|\mathbf{h}_n\|^2\cos^2\varphi_n}{1+\frac{P}{J-1}\|\mathbf{h}_n\|^2(\sin^2\varphi_n-\varepsilon)}=\frac{1+\frac{P}{J-1}\|\mathbf{h}_n\|^2(1-\varepsilon)}{1+\frac{P}{J-1}\|\mathbf{h}_n\|^2(\sin^2\varphi_n-\varepsilon)}\overset{(a)}{\cong}\frac{\frac{P}{J-1}\|\mathbf{h}_n\|^2(1-\varepsilon)}{\frac{P}{J-1}\|\mathbf{h}_n\|^2(\sin^2\varphi_n-\varepsilon)}, \tag{20}$$

where (a) follows from $\frac{P}{J-1}\|\mathbf{h}_n\|^2(\sin^2\varphi_n-\varepsilon)\gg 1$ and $\frac{P}{J-1}\|\mathbf{h}_n\|^2(1-\varepsilon)\gg 1$ in the high SNR regime, and thus the throughput (15) is rewritten as

$$R=\mathbb{E}\left[\max_{1\le i\le I}\sum_{j=1}^{J-1}\log\left(\max_{n\in\mathcal{S}_{i,j}}\frac{1-\varepsilon}{\sin^2\varphi_n-\varepsilon}\right)\right]. \tag{21}$$

The asymptotic scaling law of the throughput given by (17) is obtained as follows.

Theorem 2: *In the high SNR regime, the throughput of the spectrum sharing SDMA scales like*

$$\lim_{N\to\infty}\frac{R}{\log N}=1. \tag{22}$$

Proof : See Appendix 6.5. ∎

Thorem 2 implies that the throughput does not increases with the number of transmit antennas J. When compared to PU2RC ($\lim_{N\to\infty}\frac{R}{\frac{J}{J-1}\log N}=1$) [22], the throughput the

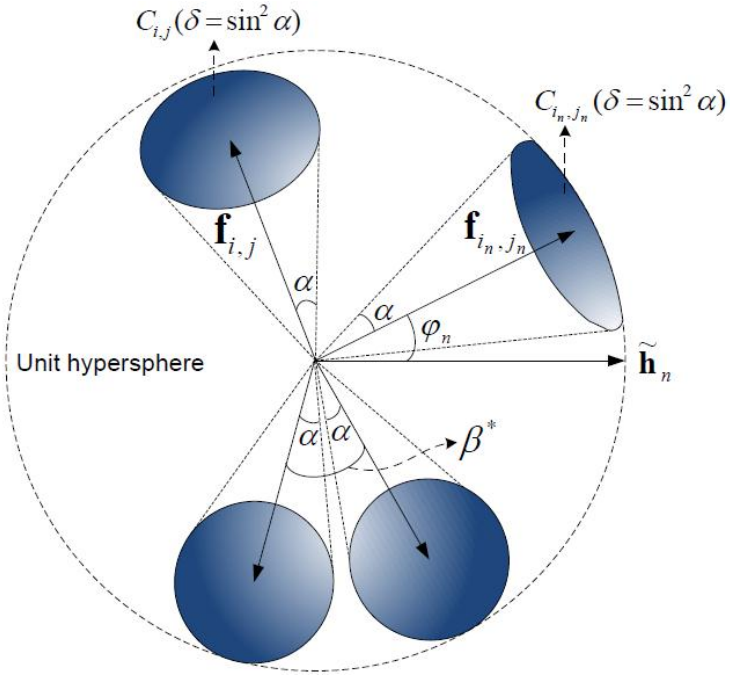

(a) $\delta \leq \delta_0$

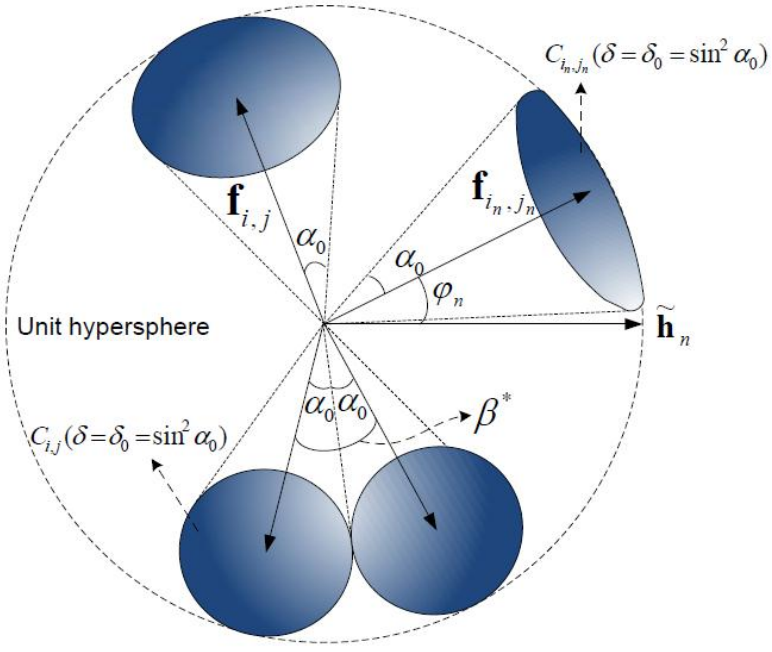

(b) $\delta = \delta_0$

Fig. 4. Channel direction $\tilde{\mathbf{h}}_n$ and its quantized channel direction $\mathbf{f}_{i_n,j_n}$. The blue surface on the unit hypersphere including $\mathbf{f}_{i,j}$ is a spherical cap $\mathcal{C}_{i,j}(\sin^2\delta)$. All surface areas are the same. (a) All spherical caps do not overlap. (b) As δ increases, two spherical caps associated with two precoding vectors forming the minimum angle β^* border each other, where $\beta^* = 2\alpha_0$ and $\alpha_0 > \alpha$.

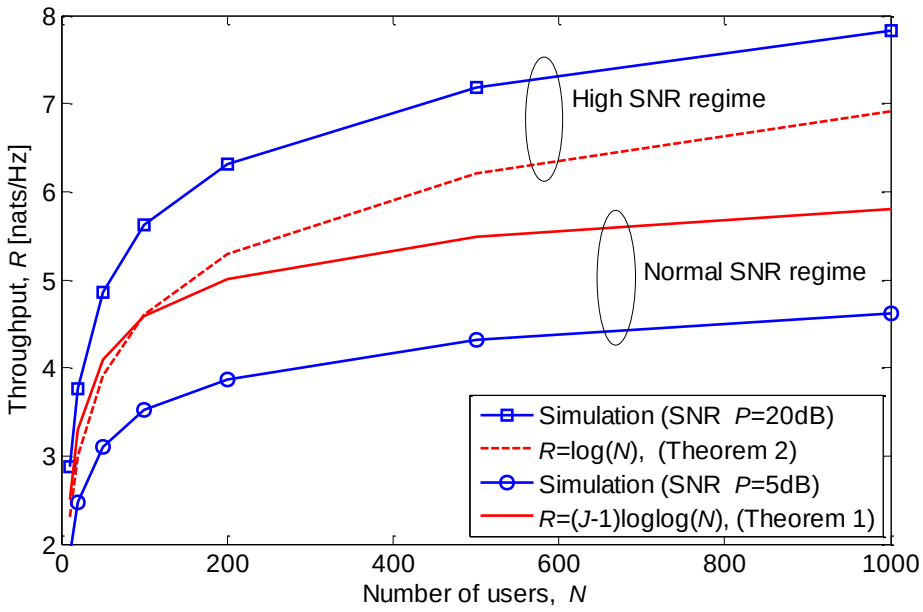

Fig. 5. Throughput R versus the number of users N for the number of precoding matrices $I = 4$, and the number of transmit antennas $J = 4$.

scaling law of the spectrum sharing SDMA is $(J-1)/J$ times that of PU2RC. Thus, the spectrum sharing SDMA achieves smaller multiplexing gain, 1, than PU2RC, $J/(J-1)$. This is due to the fact that one spatial degrees of freedom among J spatial degrees of freedoms is used for interference mitigation, and the remaining spatial degrees of freedom are devoted to send data streams. Furthermore, Theorem 2 yields a different multiuser diversity gain factor logN as compared to loglogN in Theorem 1. This is because at high SNR the throughput of the spectrum sharing SDMA is determined by the minimum quantization error, $\min_{1\le n\le N}\sin^2\varphi_n$, as shown in (33) and (38). Specifically, $\min_{1\le n\le N}\sin^2\varphi_n$ scales as $N^{-1/(J-1)}$; thus the throughput of the spectrum sharing SDMA, which is given by $(J-1)\mathbb{E}\left[-\log\left(\min_{1\le n\le N}\sin^2\varphi_n\right)\right]$, scales as $-(J-1)\log\left(N^{-1/(J-1)}\right)=\log N$. Moreover, the multiuser diversity gain factor of the spectrum sharing SDMA is identical to that of PU2RC, which indicates that no loss of the multiuser diversity gain is provided even in the high SNR regime.

4. Numerical Results

Fig. 5 shows that as the number of users increases, simulated throughput becomes parallel theoretic curve of asymptotic throughput scaling laws proclaimed in Theorems 1 and 2. This verifies the accuracy of the throughput scaling analysis. First, Theorems 1 and 2 state that the scaling law of the spectrum sharing SDMA is $(J-1)/J$ times that of PU^{2}RC that is a typical SDMA with orthogonal beamforming but not transmit null steering. Thus, the proposed scheme provides smaller multiplexing gain (which is $J-1$ for normal SNR regime, and 1 for high SNR regime) than PU^{2}RC (J for normal SNR regime, and $J/(J-1)$ for high SNR regime [22]). This is because the proposed scheme consumes one spatial degrees of freedom among total available spatial degrees of freedoms of J to mitigate the interference toward other

coexisting services, and $J-1$ spatial degrees of freedom are utilized for sending data streams. These results indicate that increasing J reduces the loss of multiplexing gain. On the other hand, the spectrum sharing SDMA requires $\log_2 I$ less feedback bits than PU^{2}RC ($\log_2 I(J-1)$ for the spectrum sharing SDMA and $\log_2 IJ$ for PU^{2}RC) .

Second, from Theorem 1 and 2, we observe that multiuser diversity increases the throughput by the factor of $\log\log N$ (normal regime) and $\log N$ (interference-limited regime), which is the same as PU^{2}RC, i.e. no loss in multiuser diversity gain. This indicates that the spectrum sharing SDMA provides the same throughput gain from opportunistic user scheduling at the transmitter multiuser compared to PU^{2}RC. The main performance metrics of the spectrum sharing SDMA versus PU^{2}RC are summarized in **Table 1.**

Table 1. The spectrum sharing SDMA vs. non-spectrum sharing SDMA (PU^{2}RC) : the number of feedback bits are independent of SNR.
$J, N, and\ I$ denotes the number of transmit antennas, users, and precoding metrices, respectively.

Performance metrics	**Normal SNR**		**High SNR**	
	Spectrum sharing SDMA	**PU^{2}RC** [22]	**Spectrum sharing SDMA**	**PU^{2}RC** [22]
Multiplexing gain factor	$J-1$	J	1	$\frac{J}{J-1}$
Multiuser diversity gain factor	$\log\log N$	$\log\log N$	$\log N$	$\log N$
Feedback bits for channel quantization	$\log_2 I(J-1)$	$\log_2 IJ$	$\log_2 I(J-1)$	$\log_2 IJ$

5. Conclusion

This paper presents the mathematical derivation of the throughput scaling laws of the spectrum sharing SDMA. Extreme value theory and uniform convergence in the weak law of large numbers are mainly applied to the derivation. The throughput scaling laws show that multiplexing gain of the proposed SDMA is $\frac{J-1}{J}$ times less than that of PU^{2}RC, whereas no loss in multiuser diversity gain. Although the spectrum sharing SDMA has lower multiplexing gain compared to PU^{2}RC in the non-coexistence scenario, it offers an intriguing opportunity to reuse spectrum already allocated to other coexisting services, and further always requires less feedback overhead than PU^{2}RC. Our results could provide insight into design fundamentals and trade-offs of the spectrum sharing SDMA. Future extension consider more realistic system model with spatially correlated channel and a theoretical analysis of the throughput loss of the spectrum sharing SDMA relative to PU^{2}RC.

6. Appendix

6.1 Proof of Lemma 1

For i-th precoding vector $\mathbf{f}_i \in \mathcal{F}, 1 \le i \le K$, we define $A(\mathcal{C}_i(\delta))$ as the surface area of a spherical cap $\mathcal{C}_i(\delta)$ on the unit hypersphere, where the cap is defined as

$$\mathcal{C}_i(\delta) = \left\{\tilde{\mathbf{h}}: 1 - \left|\tilde{\mathbf{h}} \cdot \mathbf{f}_i\right| \le \delta\right\}, 0 \le \delta \le 1. \tag{23}$$

From [29, Lemma 4], the surface area is given as $A(\mathcal{C}_i(\delta)) = 2\pi^J \delta^{J-1}/(J-1)!$, and $A(\mathcal{C}_i(1))$ is the entire surface area of the hypersphere. Then the CCDF of $\sin^2\varphi_n$is given as

$$\begin{aligned}\mathbb{P}[\sin^2\varphi_n \geq \delta] &= 1 - \frac{A\left(\cup_{i=1}^{K} \mathcal{C}_i(\delta)\right)}{A(\mathcal{C}_i(1))} \\ &\overset{(a)}{=} 1 - \frac{\sum_{i=1}^{K} A(\mathcal{C}_i(\delta))}{A(\mathcal{C}_i(1))} \\ &= 1 - K\delta^{N-1}, 0 \leq \delta \leq \delta_0,\end{aligned} \tag{24}$$

where (a) holds for x that is less than the maximum value δ_0 where all spherical caps do not overlap. In **Fig. 4** (a) and (b), the minimum angle between the precoding vectors $\{\mathbf{f}_i\}_{i=1,\cdots,K}$ is given by

$$\beta^* = \min_{1\leq i\leq j\leq M} \angle(\mathbf{f}_i, \mathbf{f}_j)\,. \tag{25}$$

Moreover, δ_0 is

$$\begin{aligned}\delta_0 &= \sin^2\alpha_0 \\ &\overset{(a)}{=} \sin^2\frac{\beta^*}{2} \\ &= 0.5(1-\cos\beta^*) \\ &\overset{(b)}{=} 0.5\left(1-\cos\left(\min_{1\leq i\leq j\leq M}\angle(\mathbf{f}_i,\mathbf{f}_j)\right)\right) \\ &= 0.5\left(1-\max_{1\leq i\leq j\leq M}\cos\left(\angle(\mathbf{f}_i,\mathbf{f}_j)\right)\right) \\ &= 0.5\left(1-\max_{1\leq i\leq j\leq M}\left|\mathbf{f}_i^{\dagger}\cdot\mathbf{f}_j\right|\right),\end{aligned}$$

where (a) follows from $\alpha_0 = \beta^*/2$, and (b) follows from (25).

6.2 Proof of Lemma 2

A major part of this proof is presented in Appendix III in [31]. From tha fact that $\mathbb{E}[X] = \int_0^1 \mathbb{P}[X > x]dx$ for $X > 0$, we obtain

$$\begin{aligned}\mathbb{E}[-\log Z] &= \int_0^\infty \mathbb{P}[Z \leq e^{-z}]dz \\ &= \int_0^\infty 1-\left(1-e^{-z(J-1)}\right)^N dz \\ &= \int_0^\infty 1-\sum_{k=0}^{N}\binom{N}{k}(-1)^k e^{-z(J-1)k}dz \\ &= \int_0^\infty \sum_{k=1}^{N}\binom{N}{k}(-1)^{k+1}e^{-z(J-1)k}dz \\ &= \sum_{k=1}^{N}\binom{N}{k}(-1)^{k+1}\int_0^\infty e^{-z(J-1)k}dz \\ &= \frac{1}{J-1}\sum_{k=1}^{N}\binom{N}{k}\frac{(-1)^{k+1}}{k} \\ &= \frac{1}{J-1}\sum_{k=1}^{N}\frac{1}{k}\,.\end{aligned} \tag{26}$$

From $\log N = \int_1^N \frac{1}{x}dx$, we obtain

$$\log N \le \sum_{k=1}^{N} \frac{1}{k} \le 1 + \log N \ . \tag{27}$$

Combining (26) and (27) completes the proof.

6.3 Proof of Lemma 3

From Lemma 1, the CCDF of X is given as

$$\mathbb{P}[X \ge x] = (1 - Kx^{J-1})^N, \ 0 \le x \le x_0 \tag{28}$$

Denote Y as the random variable with following CCDF:

$$\mathbb{P}[Y \ge y] = \begin{cases} (1 - Ky^{J-1})^N \ , & 0 \le y \le x_0 \\ \left(1 - Kx_0^{J-1}\right)^N & y \ge x_0 \end{cases} \tag{29}$$

Since a CCDF is a monotonically decreasing function, $\mathbb{P}[X \ge x] \le \left(1 - Kx_0^{J-1}\right)^N$ for $x \ge x_0$. Thus, we have

$$\mathbb{P}[X \le e^{-x}] \ge 1 - \left(1 - Kx_0^{J-1}\right)^N, x \le -\log x_0 \tag{30}$$

From (28) and (29), the expectation of the logarithm of X is

$$\begin{aligned} \mathbb{E}[-\log X] &\overset{(a)}{=} \int_0^\infty \mathbb{P}[X \le e^{-x}]dx \\ &= \int_0^\infty \mathbb{P}[X \le e^{-x}]dx + \int_{-\log x_0}^\infty 1 - \left(1 - Ke^{-x(J-1)}\right)^N dx \\ &\overset{(b)}{\ge} \int_0^{-\log x_0} 1 - \left(1 - Kx_0^{J-1}\right)^N dx + \int_{-\log x_0}^\infty 1 - \left(1 - Ke^{-x(J-1)}\right)^N dx \\ &= \mathbb{E}[-\log Y], \end{aligned} \tag{31}$$

where (a) follows from $\mathbb{E}[X] = \int_0^1 \mathbb{P}[X > x]dx$, and (b) is obtained from (30).

Next, let Z be the minimum of N independent beta $(J-1,1)$ random variables, and the CCDF of Z is $\mathbb{P}[Z \ge z] = (1 - z^{J-1})^N, 0 \le z \le 1$ [30, Lemma 1]. From (28), (29), and the CCDF of Z, the random variable $\bar{X} \triangleq K^{\frac{1}{J-1}}X, \bar{Y} \triangleq K^{\frac{1}{J-1}}Y$ and Z have the same distribution for $X, Y \in [0, x_0]$. The equivalence and (31) results in

$$\begin{aligned} \mathbb{E}[-\log\bar{X}] \ge \mathbb{E}[-\log\bar{Y}] &= \mathbb{E}[-\log Z] - \mathbb{E}[-\log Z \, , z_0 \le Z \le 1] - \frac{\log K}{J-1} - \log x_0 \\ &\overset{(a)}{\ge} \mathbb{E}[-\log Z] + \log z_0 - \frac{\log K}{J-1} - \log x_0 \\ &\overset{(b)}{\ge} \frac{\log N}{J-1}, \end{aligned} \tag{32}$$

where $z_0 = x_0 K^{\frac{1}{J-1}}$, and (a) follows the inequality:

$$\begin{aligned}\mathbb{E}[-\log Z, z_0 \le Z \le 1] &= \int_0^{-\log z_0} 1-\left(1-e^{-z(J-1)}\right)^N dz \\ &\le \int_0^{-\log z_0} 1\, dz \\ &= -\log z_0, \end{aligned} \tag{33}$$

and (b) is obtained from the lower bound in Lemma 2. This gives the desired lower bound.

Next, we obtain

$$\begin{aligned}\mathbb{E}[-\log\bar{X}] &\le \mathbb{E}[-\log\bar{X}\,|0 \le X \le x_0] \\ &= \mathbb{E}\left[-\log Z, 0 \le Z \le x_0 K^{\frac{1}{J-1}}\right] \\ &\le \frac{\mathbb{E}[-\log Z]}{\mathbb{P}\left[0\le Z\le x_0 K^{\frac{1}{J-1}}\right]} \\ &\overset{(a)}{\le} \frac{1+\log N}{(J-1)\tau}, \end{aligned} \tag{34}$$

where (a) is obtained from the upper bound in Lemma 2, and $\tau = \mathbb{P}[0 \le Z \le x_0 K^{\frac{1}{J-1}}] = 1-\left(1-Kx_0^{J-1}\right)^K$. This proves the desired upper bound.

6.4 Proof of Theorem 1

From (15) the upper bound for R is given as

$$\begin{aligned} R &= \max_{1\le i\le I}\mathbb{E}\left[\sum_{j=1}^{J-1}\log\left(\max_{n\in\mathcal{S}_{i,j}}\frac{1+\frac{P}{J-1}\|\mathbf{h}_n\|^2(1-\varepsilon)}{1+\frac{P}{J-1}\|\mathbf{h}_n\|^2(\sin^2\varphi_n-\varepsilon)}\right)\right] \\ &\le \mathbb{E}\left[\sum_{j=1}^{J-1}\log\left(\max_{1\le i\le I}\max_{n\in\mathcal{S}_{i,j}}\frac{1+\frac{P}{J-1}\|\mathbf{h}_n\|^2(1-\varepsilon)}{1+\frac{P}{J-1}\|\mathbf{h}_n\|^2(\sin^2\varphi_n-\varepsilon)}\right)\right] \\ &\overset{(a)}{\le} \mathbb{E}\left[\sum_{j=1}^{J-1}\log\left(\max_{1\le i\le I}\max_{n\in\mathcal{S}_{i,j}}1+\frac{P}{N-1}\|\mathbf{h}_n\|^2\right)\right] \\ &= (J-1)\mathbb{E}\left[\log\left(1+\frac{P}{J-1}\max_{1\le n\le N}\|\mathbf{h}_n\|^2\right)\right] \\ &\overset{(b)}{\le} (J-1)\log\left(1+\frac{P}{J-1}\left(\log N+O(\log\log N)\right)\right)\mathbb{P}\left[\max_{1\le n\le N}\|\mathbf{h}_n\|^2 \le \log N+O(\log\log N)\right] \\ &\quad +\log\left(1+\frac{P}{J-1}N\right)\mathbb{P}\left[\max_{1\le n\le N}\|\mathbf{h}_n\|^2 \ge \log N+O(\log\log N)\right] \\ &\le (J-1)\left\{\log\left(1+\frac{P}{J-1}(\log N+O(\log\log N))\right)+\log(1+\frac{P}{J-1}N)O\left(\frac{1}{\log N}\right)\right\}, \end{aligned} \tag{35}$$

where (a) follows because $0 \le \varepsilon < 1$ and $1+\frac{P}{J-1}\|\mathbf{h}_n\|^2(\sin^2\varphi_n-\varepsilon) \ge 1$, and (b) uses the asymptotic behavior of $\max_{1\le n\le N}\|\mathbf{h}_n\|^2$ given by [18, eq.(A10)]

$$\mathbb{P}\left[\left|\max_{1\le n\le N}\|\mathbf{h}_n\|^2-\log N\right| \le O(\log\log N)\right] \ge 1-O\left(\frac{1}{\log N}\right). \tag{36}$$

From (35), we have

$$\lim_{N\to\infty} \frac{R}{(J-1)\log\log N} \leq 1. \tag{37}$$

Next, from (15) the lower bound for R is given as

$$\begin{aligned} R &= \max_{1\leq i\leq I} \mathbb{E}\left[\sum_{j=1}^{J-1} \log\left(\max_{n\in\mathcal{S}_{i,\mathrm{j}}} \frac{1+\frac{P}{J-1}\|\mathbf{h}_n\|^2(1-\varepsilon)}{1+\frac{P}{J-1}\|\mathbf{h}_n\|^2(\sin^2\varphi_n-\varepsilon)}\right)\right] \\ &\overset{(a)}{\geq} \max_{1\leq i\leq I} \mathbb{E}\left[\sum_{j=1}^{J-1} \log\left(\max_{n\in\mathcal{S}_{i,j}} \frac{1+\frac{P}{J-1}\|\mathbf{h}_n\|^2}{1+\frac{P}{J-1}\|\mathbf{h}_n\|^2\sin^2\varphi_n}\right)\right] \\ &\geq \mathbb{E}\left[\sum_{j=1}^{J-1} \log\left(\max_{n\in\mathcal{S}_{i,j}} \frac{1+\frac{P}{J-1}\|\mathbf{h}_n\|^2}{1+\frac{P}{J-1}\|\mathbf{h}_n\|^2\sin^2\varphi_n}\right)\right] \\ &\overset{(b)}{\geq} (J-1)\log\left(\frac{1+\frac{P}{J-1}(\log N - O(\log\log N))}{1+\frac{P}{J-1}\left(1+\frac{O(\log\log N)}{\log N}\right)}\right)\left(1-\frac{1}{2(\log N)^{J-1}}\right)\left(1-O\left(\frac{1}{\log N}\right)\right), \end{aligned} \tag{38}$$

where (a) follows from

$$\begin{aligned} &\frac{1+\frac{P}{J-1}\|\mathbf{h}_n\|^2(1-\varepsilon)}{1+\frac{P}{J-1}\|\mathbf{h}_n\|^2(\sin^2\varphi_n-\varepsilon)} \Big/ \frac{1+\frac{P}{J-1}\|\mathbf{h}_n\|^2}{1+\frac{P}{J-1}\|\mathbf{h}_n\|^2\sin^2\varphi_n} \\ &= \frac{1+\frac{P}{J-1}\|\mathbf{h}_n\|^2(\sin^2\varphi_n-\varepsilon)+\frac{P}{J-1}\|\mathbf{h}_n\|^2+\left(\frac{P}{J-1}\|\mathbf{h}_n\|^2\right)^2\sin^2\varphi_n-\left(\frac{P}{J-1}\|\mathbf{h}_n\|^2\right)^2\sin^2\varphi_n\varepsilon}{1+\frac{P}{J-1}\|\mathbf{h}_n\|^2(\sin^2\varphi_n-\varepsilon)+\frac{P}{J-1}\|\mathbf{h}_n\|^2+\left(\frac{P}{J-1}\|\mathbf{h}_n\|^2\right)^2\sin^2\varphi_n-\left(\frac{P}{J-1}\|\mathbf{h}_n\|^2\right)^2\varepsilon} \\ &\geq \frac{1+\frac{P}{J-1}\|\mathbf{h}_n\|^2(\sin^2\varphi_n-\varepsilon)+\frac{P}{J-1}\|\mathbf{h}_n\|^2+\left(\frac{P}{J-1}\|\mathbf{h}_n\|^2\right)^2\sin^2\varphi_n-\left(\frac{P}{J-1}\|\mathbf{h}_n\|^2\right)^2\varepsilon}{1+\frac{P}{J-1}\|\mathbf{h}_n\|^2(\sin^2\varphi_n-\varepsilon)+\frac{P}{J-1}\|\mathbf{h}_n\|^2+\left(\frac{P}{J-1}\|\mathbf{h}_n\|^2\right)^2\sin^2\varphi_n-\left(\frac{P}{J-1}\|\mathbf{h}_n\|^2\right)^2\varepsilon} = 1 \end{aligned} \tag{39}$$

, and (b) is obtained by using the last inequality of [22, Proposition 1]. From (38), we have

$$\lim_{N\to\infty} \frac{R}{(J-1)\log\log N} \geq 1. \tag{40}$$

Combining (37) and (40) completes the proof.

6.5 Proof of Theorem 2

From (20) the upper bound for R is given as

$$\begin{aligned} R &= \mathbb{E}\left[\max_{1\leq i\leq I}\sum_{j=1}^{J-1} \log\left(\max_{n\in\mathcal{S}_{i,j}} \frac{1-\varepsilon}{\sin^2\varphi_n-\varepsilon}\right)\right] \\ &\overset{(a)}{\leq} \mathbb{E}\left[\sum_{j=1}^{J-1} \log\left(\max_{1\leq i\leq I}\max_{n\in\mathcal{S}_{i,j}} \frac{1-\varepsilon}{sin^2\varphi_n-\varepsilon}\right)\right] \\ &\overset{(b)}{\leq} \mathbb{E}\left[\sum_{j=1}^{J-1} \log\left(\max_{1\leq i\leq I}\max_{n\in\mathcal{S}_{i,j}} \frac{1}{sin^2\varphi_n-\varepsilon}\right)\right] \\ &= (J-1)\mathbb{E}\left[\log\left(\max_{1\leq n\leq N} \frac{1}{sin^2\varphi_n-\varepsilon}\right)\right] \\ &= (J-1)\mathbb{E}\left[-\log\left(\min_{1\leq n\leq N} \sin^2\varphi_n-\varepsilon\right)\right] \end{aligned}$$

$$\overset{(c)}{\leq} \frac{1+\log N}{1-\left(1-Kx_0^{J-1}\right)^N} + \log K, \tag{41}$$

where (a) is attributed the fact that the scheduling in the second line can select any precoding vectors that maximizes their throughputs among $I(J-1)$vectors in the codebook $\mathcal{F}$; that is, guaranteeing more freedom of choice results in the higher throughput. (b) follows from $0 \leq \varepsilon < 1$, and (c) is obtained from the upper bound in Lemma 3 and the fact that $\varepsilon \approx 0$ for large N. Since $\left(1-Kx_0^{J-1}\right)^N \approx 0$ and $\log N \gg 1 + \log K$ for large N, from (41) we have

$$\lim_{N\to\infty} \frac{R}{\log N} \leq 1. \tag{42}$$

For the precoding vector $\mathbf{f}_{i,j} \in \mathcal{F}$, we define a spherical cap on the unit hypersphere as $\mathcal{C}_{i,j}(\delta) = \{\tilde{\mathbf{h}} \in \mathbb{C}^J | 1 - |\tilde{\mathbf{h}} \cdot \mathbf{f}_{i,j}| \leq \delta\}, 0 \leq \delta \leq 1$. Additionally, let define the index set of users in the sphere cap $\mathcal{C}_{i,j}(\delta_1)$ as

$$\mathcal{U}_{i,j} = \{1 \leq n \leq N | \tilde{\mathbf{h}}_n \in \mathcal{C}_{i,j}(\delta_1)\}, \tag{43}$$

where δ_1 is the maximum distance of the codebook $\mathcal{F}$ defined as $\delta_1 = 0.5\max_{1\leq i\leq j\leq K} 1 - |\mathbf{f}_i^\dagger \cdot \mathbf{f}_j|$. We then have $\min_{n\in\mathcal{S}_{i,j}} \sin^2\varphi_n = \min_{n\in\mathcal{U}_{i,j}} \sin^2\varphi_n$. From (20) the lower bound for R is given by

$$\begin{aligned} R &= \mathbb{E}\left[\max_{1\leq i\leq I} \sum_{j=1}^{J-1} \log\left(\max_{n\in\mathcal{S}_{i,j}} \frac{1-\varepsilon}{\sin^2\varphi_n - \varepsilon}\right)\right] \\ &\overset{(a)}{\geq} \mathbb{E}\left[\max_{1\leq i\leq I} \sum_{j=1}^{J-1} \log \max_{n\in\mathcal{S}_{i,j}} \frac{1}{\sin^2\varphi_n}\right] \\ &\overset{(b)}{\geq} \mathbb{E}\left[\sum_{j=1}^{J-1} \log \max_{n\in\mathcal{S}_{i,j}} \frac{1}{\sin^2\varphi_n}\right] \\ &= \mathbb{E}\left[\sum_{j=1}^{J-1} -\log \min_{n\in\mathcal{S}_{i,j}} \sin^2\varphi_n\right] \\ &= \mathbb{E}\left[\sum_{j=1}^{J-1} -\log \min_{n\in\mathcal{U}_{i,j}} \sin^2\varphi_n\right] \end{aligned} \tag{44}$$

where (a) follows from $\frac{1-\varepsilon}{\sin^2\varphi_n - \varepsilon} \geq \frac{1}{\sin^2\varphi_n}$ for $0 \leq \varepsilon < 1$. (b) follows from that the third line has no selection of the precoding matrix that maximizes the sum throughput, which results in the lower throughput. The number of user contained in the set $\mathcal{U}_{i,j}$ satisfies the following inequality [22, Lemma 1]:

$$\mathbb{P}\left[|\mathcal{U}_{i,j}| \geq \delta_1^{J-1} N - 1\right] \geq 1 - N^{-1}, \tag{45}$$

where the parameters of [22, Lemma 1] are substituted as $U = N$, $A = \delta_1^{J-1}$, and $\tau_1 = \tau_2 = N^{-1}$. From (41) and (42),

$$R \geq (J-1)\mathbb{E}\left[-\log \min_{n\in\mathcal{U}_{i,j}} \sin^2\varphi_n \,\middle|\, |\mathcal{U}_{i,j}| \geq \delta_1^{J-1} N - 1\right](1 - N^{-1}). \tag{46}$$

Applying the lower bound in Lemma 3 to this, we have

$$R \geq \left(\log(\delta_1^{J-1}N - 1) + \log K\right)(1 - N^{-1}). \tag{47}$$

Since $\log N \gg \log K$ and $\log N \gg \log \delta_1^{J-1}$ for large N, from (47) we have

$$\lim_{N\to\infty} \frac{R}{\log N} \geq 1. \tag{48}$$

Combining (42) and (48) completes the proof.

References

[1] J. Chen, X. Zhang, and Y. Kuo, "Adaptive Cooperative Spectrum Sharing Based on Fairness and Total Profit in Cognitive Radio Networks," *ETRI Journal*, vol.32, no.4, pp 512-519, August 2010. Article (CrossRef Link)

[2] H.-S. Jo, C. Mun, J. Moon, and J.-G. Yook, "Interference mitigation using uplink power control for two-tier femtocell networks," *IEEE Trans. on Wireless Commun.*, vol. 8, no. 10, pp. 4906-4910, October 2009. Article (CrossRef Link)

[3] H.-S. Jo, Y. J. Sang, P. Xia, and J. G. Andrews, "Heterogeneous cellular networks with flexible cell association: a comprehensive downlink SINR analysis," *IEEE Trans. on Wireless Commun.,* vol. 11, no. 10, pp. 3484-3495, Oct. 2012. Article (CrossRef Link)

[4] A. Ghosh, N. Mangalvedhe, R. Ratasuk, B. Mondal, M. Cudak, E. Visotsky, T. A Thomas, J. G Andrews, P. Xia, H.-S. Jo, H. S Dhillon, T. D Novlan,"Heterogeneous cellular networks: From theory to practice," *IEEE Communications Magazine*, vol. 50, no. 6, pp. 54-64, June 2012. Article (CrossRef Link)

[5] IST-4-027756 WINNER II D 5.10.1. "The WINNER role in the ITU process towards IMTAdvanced and newly identified spectrum", vol. 1.0, November 2007.

[6] ITU-R WP 8F/TEMP/290, "Preliminary draft new report on radio aspects for the terrestrial component of IMT-2000 and systems beyond IMT-2000", October 2005.

[7] 3GPP, "FDD RIT component of SRIT LTE Release 10 & beyond (LTE-Advanced)," RP-090739, September 2009.

[8] H.-S. Jo, C. Mun, J. Moon, and J.-G. Yook, "Self-optimized coverage coordination and coverage analysis in femtocell networks," *IEEE Trans. on Wireless Commun.*, vol. 9, no. 10, pp. 2977-2982, October 2010. Article (CrossRef Link)

[9] T. A. Weiss and F. K. Jondral "Spectrum pooling: an innovative strategy for the enhancement of spectrum efficiency," *IEEE Communications Magazine*, vol. 42, no. 3, pp. S8-14, March 2004. Article (CrossRef Link)

[10] B. Friedlander and B. Porat, "Performance analysis of a nullsteering algorithm based on direction-of-arrival estimation," *IEEE Trans. on Acoustic, Speech, Signal Processing*, vol. 37, pp. 461-466, April 1989. Article (CrossRef Link)

[11] H.-S. Jo, H.-G. Yoon, J. Lim, Y.-H. Park, J.-G. Yook, "Coexistence Method to Mitigate Interference from IMT-Advanced to Fixed Satellite Service," *Wireless Technologies, European Conf., 2007*, pp. 158-161. Article (CrossRef Link)

[12] V. Asghari and S. Aissa, "Resource Management in Spectrum-Sharing Cognitive Radio Broadcast Channels: Adaptive Time and Power Allocation," *IEEE Trans. Commun.*, vol.59, no.5, pp.1446- 1457, May 2011. Article (CrossRef Link)

[13] D. I. Kim, L. Le, and E. Hossain,, "Joint rate and power allocation for cognitive radios in

dynamic spectrum access environment," *IEEE Trans. Wireless Commun*., vol. 7, no. 12, pp. 5517-5527, Dec. 2008. Article (CrossRef Link)
[14] A. T. Hoang and Y.-C. Liang, "Downlink channel assignment and power control for cognitive radio networks," *IEEE Trans. Wireless Commun*., vol. 7, no. 8, pp. 3106-3117, Aug. 2008. Article (CrossRef Link)
[15] X. Gong and G. Ascheid, "Ergodic Capacity for Cognitive Radio with Partial Channel State Information of the Primary User," *IEEE Wireless Communications and Networking Conference (WCNC)*, pp.555-560, April 2012. Article (CrossRef Link)
[16] A. Ghasemi and E. S. Sousa, "Fundamental limits of spectrum sharing in fading environments," *IEEE Trans. on Wireless Commun*., vol. 6, no. 2, pp. 649–658, Feb. 2007. Article (CrossRef Link)
[17] H. Weingarten, Y. Steinberg, and S. Shamai (Shitz), "The capacity region of the Gaussian MIMO broadcast channel," *in Proc. IEEE ISIT*, June 2004. Article (CrossRef Link)
[18] M. Sharif, and B. Hassibi, "On the capacity of MIMO broadcast channel with partial side information," *IEEE Trans. on Information Theory*, vol. 51, no. 2, pp. 506-522, February 2005. Article (CrossRef Link)
[19] T. Yoo, N. Jindal, and A. Goldsmith, "Multi-antenna downlink channels with limited feedback and user selection," *IEEE J. Sel. Areas Commun*., vol. 25, no. 7, pp. 1478-1491, July 2007. Article (CrossRef Link)
[20] Samsung Electronics, "Downlink MIMO for EUTRA," in 3GPP TSG RAN WG1 R1-060335., February 2006.
[21] 3GPP2, "Physical layer for ultra mobile broadband (UMB) air interface specification," in 3GPP2 C.S0084-001-0., April 2007.
[22] K. Huang, J. G. Andrews, and R. W. Heath, "Performance of orthogonal beamforming for SDMA with limited feedback," *IEEE Trans. on Vehicular Technolgy*, vol.58, no.1, pp.152-164, Jan. 2009. Article (CrossRef Link)
[23] T. H. Kim, R. W. Heath, and S. Choi, "Multiuser MIMO Downlink with Limited Feedback Using Transmit-Beam Matching," *IEEE International Conference on Commun*., vol., no., pp.3506-3510, 19-23 May 2008. Article (CrossRef Link)
[24] S.A.Sattarzadeh and A. Olfat, "Bounds on the Throughput Performance of PU2RC and Its Application in Mode Switching," *IEEE Trans on Vehicular Technology*, vol.61, no.2, pp.876-882, Feb. 2012. Article (CrossRef Link)
[25] H.-S. Jo, "Codebook-Based Precoding for SDMA-OFDMA with Spectrum Sharing", *ETRI Journal*, vol. 33, no. 6, pp.831-840, Dec. 2011. Article (CrossRef Link)
[26] 3rd Generation Partnership Project, Spatial channel model for multiple input multiple output MIMO simulations, vol. TR 25.996, v10.1.0, 2011.
[27] Jeffrey. A. Fessler and Alfred O. Hero, "Space-alternating generalized expectation-maximization algorithm," *IEEE Trans. on Signal Process*., vol.42, no.10, pp.2664-2677, Oct Spec1994. Article (CrossRef Link)
[28] P. Chevalier, A. Ferreol, and L. Albera, "High-Resolution direction finding from higher order statistics: The 2q-MUSIC algorithm," *IEEE Trans. on Signal Process*., vol. 54, no. 8, pp. 2986-2997, Aug. 2006. Article (CrossRef Link)
[29] K. K. Mukkavilli, A. Sabharwal, E. Erkip, and B. Aazhang, "On beamforming with finite rate feedback in multiple-antenna systems," *IEEE Trans. on Information Theory*, vol. 49, no. 10, pp. 2562-2579, Oct.r 2003. Article (CrossRef Link)
[30] C. Au-Yeung and D. J. Love, "On the performance of random vector quantization limited feedback beamforming in a MISO system," *IEEE Trans. on Wireless Commun*., vol. 6, no. 2, pp. 458-462, Feb. 2007. Article (CrossRef Link)
[31] N. Jindal, "MIMO broadcast channels with finite-rate feedback," *IEEE Trans. on Information Theory*, vol. 52, no. 11, pp. 5045-5060, Nov. 2006. Article (CrossRef Link)

Han-Shin Jo is an Assistant Professor with the Department of Electronics and Control Engineering, Hanbat National University in Korea. He was a Postdoctoral Research Fellow in Wireless Networking and Communications Group, the Department of Electrical and Computer Engineering, the University of Texas at Austin from 2009-11. He developed LTE systems in Samsung Eletronics in 2011-12. He received the B.S., M.S., and Ph.D. degrees in Electrical and Electronics Engineering from Yonsei University Seoul, Korea, in 2001, 2004, and 2009, respectively. He received 2011 ETRI Journal Award. His research interests include Small cells, Heterogeneous network, Massive MIMO, Stochastic geometry, and Wireless broadband transmission